LiDAR aided Wireless Networks - Beam Prediction for 5G

Dileepa Marasinghe[1],Nalin Jayaweera[1], Nandana Rajatheva[1],
Sami Hakola[2], Timo Koskela[2], Oskari Tervo[2], Juha Karjalainen[2], Esa Tiirola[2], Jari Hulkkonen[2]
[1]Centre for Wireless Communications, University of Oulu, Oulu, Finland
[2]Nokia Standards, Oulu, Finland
{ dileepa.marasinghe,nalin.jayaweera, nandana.rajatheva}@oulu.fi,
{sami.hakola, timo.koskela, oskari.tervo, juha.p1.karjalainen, esa.tiirola, jari.hulkkonen}@nokia-bell-labs.com

***Abstract*—5G New Radio (NR) mmWave operates with narrow beams. Beam-based connections require careful management of beams to ensure a reliable connection, specially when the user has mobility. 5G NR beam management achieve this, at the expense of periodic reporting with increased overheads and resource usage. Concurrently, recent interest in sensing for assisting wireless systems provides an opportunity to extract situational awareness information which can aid in proactive decisions for the network. In this work, we utilize an infrastructure-mounted light detection and ranging (LiDAR) sensor system simultaneously operating with the wireless system to predict future beam decisions. A recurrent neural network (RNN) based learning model is proposed for the beam prediction, employing tracking information of users facilitated by the LiDARs and beam sequence information from the wireless system. Furthermore, a method for predictive beam management with increased periodicity of the reporting mechanism and aperiodic reporting is analyzed. The results for the considered scenario reveal 86.8% of the resources can be saved compared to the conventional beam reporting procedure, while achieving an 88.7% accuracy for optimal beam decisions.**

***Index Terms*—LiDAR, 5G, machine learning, vision aided communications, mmWave, THz.**

I. Introduction

Exploring the higher bands in the 3rd Generation Partnership Project (3GPP) 5G NR with frequency range 2 (FR2), provides a new opportunity to utilize the enormous bandwidth available in the higher frequencies which enables a plethora of applications with higher data rates and lower latency. However, several challenges exist for the communication in these bands such as higher path loss and higher scattering, which effectively reduces the coverage area. Nevertheless, the smaller wavelength allows more antennas to be packed in a compact form factor encouraging the use of multi-antenna technologies to overcome the challenges to a certain extent. These massive antenna arrays support ultra-narrow pencil beams which can concentrate the transmission power to an intended direction mitigating the effect of path loss and interference. Thus, beam-based communication is the prominent candidate for these higher frequency bands. However, these higher frequency beams are formed using the analog beamforming technology which can support only a single beam from both base station (BS) and user equipment (UE) side. Furthermore, use of these narrow beams increases the vulnerability to random blockages. Thus, one key drawback in such a beam-based system is the requirement of beam alignment which demands a significant effort from the communication system to maintain a reliable connection, specially when the user has mobility. 5G beam management procedures are designed effectively to monitor the link through periodic measurements to achieve a reliable connection at the expense of increased overhead and exhaustive search over the possible directions [1]. The BS or the access point (AP) transmits synchronization signal block (SSB) beams which are used for the initial access process by the UE. When the UE is transferred to the connected state, refining the served beam-pair to a narrower beam-pair is done from both UE and AP ends through channel state information reference signal (CSI-RS) beams. Once such a refined beam-pair is identified, the beam management procedures try to maintain the beam alignment. This is achieved through sending periodic beam measurement reports (BMR) from the UE to the AP which monitors the received power of the transmitted beams. In case of a beam misalignment due to the mobility of the user or some blockage, a new beam-pair to correct the beam misalignment is identified using the BMR. Therefore, the periodic beam measurement reporting is essential for maintaining the link quality, although it involves a high resource usage and overhead. Moreover, the 5G NR defines aperiodic CSI-RS triggering which allows on-demand BMR [1].

Alternatively, the factors effecting the beam misalignment can be proactively inferred to a satisfactory level by monitoring the environment dynamics utilizing sensing technologies. These sensing technologies facilitate positioning and tracking of users carrying the UE. Such positioning and tracking information enables the prediction of the movement trajectory, incoming blockages and line-of-sight (LOS)/Non-LOS (NLOS) transition of the users which cause the beam misalignment invoking the beam switching procedure. Recently, the research on utilization of both radio frequency (RF) sensors and non-RF sensors for aiding communication gained widespread attention. MmWave-RADARs, LiDARS and cameras are some candidate sensing technologies which are being investigated. Furthermore, a new study item [2] has been established in SA1 working group which is responsible for the service and

system aspects of the Release-19 in the 3GPP standard to incorporate sensing to provide new services and enhancements to the communication system. Moreover, 3GPP RAN1-led Rel-18 study item on artificial intelligence/machine learning for NR air interface will also consider beam prediction as one use case of exploiting machine learning in the air interface [3]. Motivated by these factors and the ability to provide detailed yet privacy-persevered data, we employ LiDAR as the sensing modality in this work. We consider an infrastructure-mounted LiDAR system following our previous works [4], [5], [6] for beam prediction assisting a 5G NR system. We focus on predicting the future downlink beams while reducing the frequency of the beam reports, thus reducing the resource usage for beam measurements.

The paper is organized as follows. Section II discusses the related work on beam prediction. The proposed LiDAR aided beam prediction method is described in Section III and in Section IV, we describe the details of the evaluated scenario and the data generation methods. Section V presents the simulation results and discusses the improvements identified. Section VI concludes the paper.

II. Previous work

The use of LiDAR data to enhance the beam selection and prediction has been discussed in [7],[8] and [9]. Authors in [7] introduce a deep learning-based beam selection in a vehicular scenario studying the LOS/NLOS classification and top-K beam selection. The same setup and two centralized schemes have been studied in [8], which concludes that the distributed architecture in [7] performs better. The authors in [9] present a novel method using convolutional neural networks (CNN) with knowledge distillation, and introduce a curriculum training approach for improved convergence. Furthermore a non-local attention module has been introduced to improve the performance in NLOS cases. The use of camera images as side information for the beam and blockage prediction is discussed in [10]. In [11] the optimal beams are predicted adopting object detection from camera images to locate the positions of the users. Then an angle prediction model has been used to estimate the angles between the users and the cameras which is finally used for beam selection from a predefined code book.

Use of an RNN for the beam prediction task is reported in [12] where the beam prediction problem has been considered as a sequence generation problem. A sequence-to-sequence (Seq2Seq) model has been proposed and the prediction model confidence is used for assessing the beam accuracy with refinement from 5G beam management procedures.

III. LiDAR aided beam prediction

We utilize an infrastructure-mounted LiDAR system which provides 3D information on the communication environment, to predict beam decisions for the future instances. This reduces the need of frequent conventional measurement-based beam selection procedure which saves a significant amount of RF resources. The motivation arises since the requirement for beam switching occurs infrequently compared to the frequency of the CSI-RS periodic BMR, unless the UE is travelling at very high speeds or there are rapid variations in the blockage conditions. We consider a low mobility scenario such as in an indoor environment which also facilitates user detection and tracking using the deployed LiDAR sensors and utilize the data for predicting the future beams for the connected users. The location information of a UE which can be extracted from the LiDAR data, has a high correlation with the beam that is required to serve the UE. This correlation further expands in the temporal dimension resulting in a beam sequence corresponding to the trajectory of the UE. Thus the trajectory history of a user implies the future movement pattern can be utilized for the proactive beam decisions.

A. System model

An indoor scenario is considered with a single access point (AP) serving the users in the higher frequencies (i.e. mmWave / THz) with beam-based connections. The AP consists of N antennas which are uniform planar arrays (UPA), each supporting analog beamforming with a beam codebook of M beams, mounted at an elevated position (e.g. on the ceiling) with a mechanical tilt such that the UEs on the indoor area can be served. For simplicity, humans who are moving or static within the indoor area carrying single-antenna UEs are considered. The initial connections between the UEs and the AP are assumed to be established in the initial access phase. The AP selects the serving beams based on the 5G beam management procedure using the beam sweeping and periodic BMRs as described in Section I. For simplicity, the beam selection procedure is abstracted with selecting a beam index $b_u^t \in \{0, ..., M \times N\}$ at the t-th time instance for the u-th user. The position of the u-th user in the considered area at the t-th time instance is denoted by $\mathbf{p}_u^t = [x_u^t \; y_u^t]^T$.

A co-existing LiDAR system with L LiDAR sensors mounted to monitor the indoor area is considered. These LiDAR sensors are connected to a central computing unit in the system which processes the captured point cloud data for detection and tracking of users visible in the area. Then the tracking information is communicated to the AP though a back-haul connection. Prior to the operation, the static background environment is mapped using the LiDAR sensors and stored as the global map $\mathbf{c}^0 \in \Re^{V \times 3}$, which does not contain any users, where V is the number of points in the point cloud. At the time of operation, the central unit creates a combined 3D point cloud $\mathbf{c}^t$ of the total area covered by the sensors using the relative 3D transformation matrices [13] with a rate of f_l synchronized with the output rates of the sensors. This input LiDAR point cloud $\mathbf{c}^t$ is processed based on the method proposed in [14] adapted for static sensors which was also used in our prior work in [6]. When $\mathbf{c}_t$ becomes available, the algorithm first subtracts $\mathbf{c}^0$ from $\mathbf{c}^t$ to isolate the foreground points. The remaining foreground points are then clustered using Euclidean clustering and further refined using Haselich's split-merge clustering algorithm [15]. Then a Kalman filter with a constant velocity model predicts the

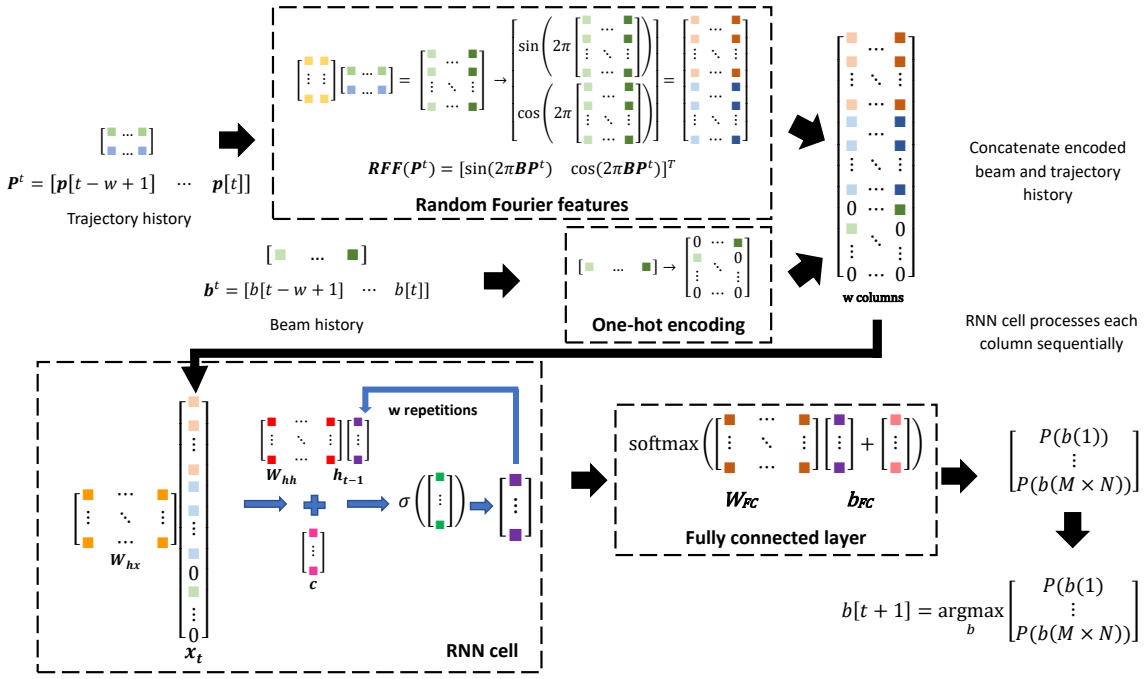

Fig. 1. Machine learning model.

position of the cluster and the nearest neighboring cluster in $\mathbf{c}^t$ is identified to keep tracking the same user in $\mathbf{c}^{t+i}$, $\forall\, i > 0$. We consider an observation window of w instances for building the beam history, $\mathbf{b}_u^t = [b_u^{t-w+1}\ b_u^{t-w+2}\ \dots\ b_u^t]$ and trajectory history, $\mathbf{P}_u^t = [\mathbf{p}_u^{t-w+1}\ \mathbf{p}_u^{t-w+2} \dots\ \mathbf{p}_u^t]^T$ extracted from $\mathbf{C}^t = [\mathbf{c}^{t-w+1}\ \mathbf{c}^{t-w+1}\ \dots\ \mathbf{c}^t]^T$. The objective of the proposed method is to predict the optimal beam index for the next time index, b_u^{t+1} such that

$$b_u^{t+1} = \underset{b\in\{0,\dots,M\times N\}}{\operatorname{argmax}} \mathbb{P}(b_u^{t+1} = b \mid \mathbf{b}_u^t, \mathbf{P}_u^t).$$

B. Proposed prediction model

A recurrent neural network (RNN) is proposed to predict b_u^{t+1} as shown in Figure 1[1]. First, $\mathbf{b}_u^t$ is one-hot encoded and stacked for the observation window w. Then, $\mathbf{P}_u^t$ is encoded using the random Fourier features (RFF) which provide a better emphasis for the location information [16]. It has been shown that classical neural networks which use MLPs cannot capture the low-dimensional features such as raw location data. The authors in [16] demonstrated the efficiency improvement for location-aided beamforming utilizing an RFF layer. Following a similar approach for the location encoding, trajectory history for u-th user is encoded using an RFF layer. This RFF layer is a fixed layer which can be expressed as

$$RFF(\mathbf{P}_u^t) = [\cos(2\pi\mathbf{B}\mathbf{P}_u^t), \sin(2\pi\mathbf{B}\mathbf{P}_u^t)]^T, \qquad (1)$$

where $\mathbf{B} \in \Re^{R\times 2}$ with a Gaussian kernel $\mathbf{B} \sim \mathcal{N}(\mathbf{0}, s^2\mathbf{I})$ such that the variance s^2 affect the frequency range involved in the RFF. The one-hot encoded beam sequence and RFF layer output are concatenated and inputted to the RNN layer which encodes the time series data. Then the output from the RNN layer is sent to a fully connected layer with softmax activation which outputs the probability of each beam being the next beam. The most probable beam is selected as the next beam index for the considered user.

[1]Only a basic RNN cell is shown in the Figure 1 to represent the use of the RNN.

C. Predictive beam management for 5G

In this section we describe an algorithm to utilize the beam predictions from the proposed model in 5G beam management inspired from the method in [12]. At the inference mode, when a sufficient trajectory and beam history based on periodic BMRs has been accumulated, the model can start predicting the next beam index. Recall that our main objective was to reduce the frequent measurement-based beam selection or in other words increase the interval between two BMRs obtained through the beam sweeping. This can be achieved by increasing the interval between periodic beam reports and utilizing the predicted beam from the proposed model. The model also provides the confidence on its prediction which can be used to monitor the beam prediction accuracy. From the next time instance onward, the window will be updated with the latest tracking information while the oldest will be discarded. Similarly, the latest beam used will be updated in the beam history. The confidence score of the model gives the probability of a beam being the next serving beam. If the confidence score falls, this means there can be more than one beam that is suitable to be the next serving beam. Therefore, based on a threshold on the confidence score, we trigger an aperiodic CSI-RS BMR if the confidence score is less than the threshold value (δ). Here the BMR is requested for the top-k beams whose sum of the confidences scores satisfy the

threshold value. This will ensure that the best beam is selected and if none of the beams in the top-k beams meet the minimum RSRP criteria [1], the conventional 5G beam selection can be utilized or skip serving at the particular time instance.

IV. Evaluation

In this section, we present the setup for evaluation of the proposed model and the beam management algorithm using simulations with a synthetic dataset. The dataset parameters were chosen referring the 3GPP Indoor hotspot scenario[17].

A. Scenario and dataset

The dataset for evaluation of the proposed model was built using Blensor [18], a LiDAR simulator based on Blender and ray tracing for wireless channel simulations using Wireless Insite [19]. The layout of the indoor area is shown in Figure 2. The parameters used in the simulation are listed in Table I.

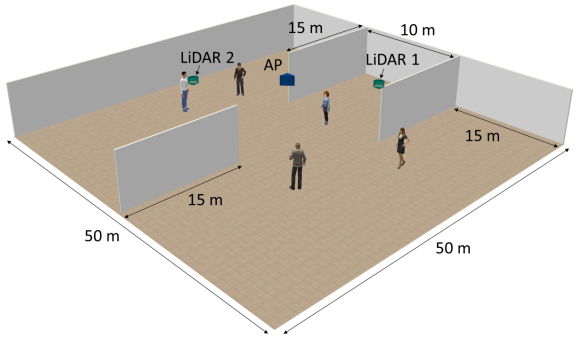

Fig. 2. Considered simulation environment

Parameter	Value
Carrier frequency	28 GHz
Bandwidth	396 MHz / 275 RBs
Subcarrier spacing	120 KHz / 0.125ms
AP antennas (N)	3 - 8x8 UPA
No. of beams per antenna (M)	64
AP and LiDAR height	3 m
Antenna boresight	$30°, 150°, 270°$
Mechanical downtilt	20
Element spacing	0.5 λ
Tx Power	20 dBm
UE antennas	Single isotropic
UE trajectories	10 per scene
Max velocity UE	0.833 m/s
No. of LiDAR sensors (L)	2
LiDAR frequency (f_l)	20 Hz

TABLE I
Simulation parameters

The user trajectories were simulated using ORCA simulator [20] where the starting and ending points are randomly selected from the corners of the layout and the user tries to reach to the opposite side of the area avoiding collision with others. We simulated 20 scenes spanning 300 frames per scene with 10 users. The positions were sampled with 100 ms intervals along the trajectory of a user. Then, the channel matrices between the positions and antennas were generated using the raytracing tool. Then, communication-based beam decisions were calculated for each position by applying the precoders for the 64 beams per antenna. The beams corresponding to the highest SNR was selected as the serving beams simulating the 5G beam selection procedure. Then each beam index was duplicated to simulate a 50 ms sampling interval which matches with the LiDAR location update running at 20 Hz. This serves as the ground truth data for training and evaluation of the model. For simulating the increased CSI-RS BMR periodicity, we simply pick generated beam index with the required multiple of the interval corresponding to the LiDAR location update frequency. Similarly, aperiodic CSI-RS BMR is simulated by picking the corresponding data for the time instance of the BMR from the ground truth data.

B. Training

We considered long short-term memory (LSTM) and gated recurrent unit (GRU) as RNNs with same hidden state dimension. Furthermore an MLP model replacing the RNN layer and a model using an MLP layer for location embedding followed by an LSTM layer were considered. All the models were trained with categorical cross-entropy loss with Adam optimizer and a 80:20 data split between train and validation sets for 10 epochs. The observation time window for the training was considered as 10 frames. The hidden state dimension was set to 32 while the RFF layer was fixed with 200 non-trainable parameters with 100 parameters per dimension, and the Gaussian kernel with a variance $s = \frac{1}{2\pi}$ after hyper-parameter tuning. We considered top-k accuracy as the evaluation metric which means the ground truth beam index is within the first k most probable beam predictions from the model for a given time index. We used leave-one-out cross-validation (LOOCV) for calculating the top-k accuracy and we average over the number of scenes which gives us an unbiased and reliable estimate of the model performance as we have a smaller dataset, which is restricted by the high computation time of ray tracing.

V. Results and Discussion

In this section, we present the performance of the considered models for the beam prediction problem, and then evaluate the predictive beam management algorithm based on the best performing model. In Figure 3, we compare the top-k accuracy of the considered models by varying the number of beams searched (k). Overall, the model with an RFF layer for location encoding and an LSTM layer (RFF+LSTM) for capturing the time series effect gives the best performance. Clearly, the sequential nature of the beam prediction problem has given better performance in all the three models using an RNN layer compared to the RFF+MLP model which uses fully connected layers only.

Next, we investigate the impact of the RFF layer. For this, we increase the periodic CSI-RS based BMR interval by multiplying the conventional BMR interval with a factor (F) and provide only the location updates from LiDAR in between the two BMRs. Therefore if $F = 4$, the conventional CSI-RS BMRs are sent every 4-th time instance. The system relies on the past predicted indices and the location update from the

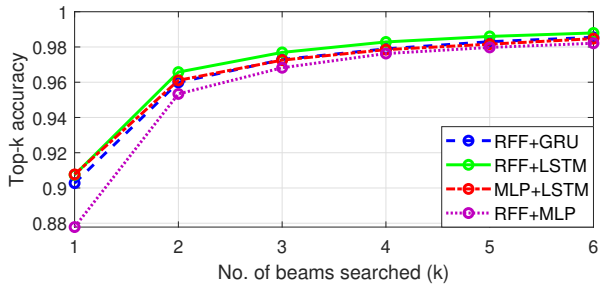

Fig. 3. Top-k accuracy vs No. of beams searched (k)

LiDAR data to predict the next beam index for the rest of the time instances. In Figure 4, we plot the top-1 accuracy of the RNN models (with and without RFF layer) and the proposed method in [12], which employs a Seq2Seq model (beam-only) utilizing only the beam sequence data. Both RFF+LSTM and

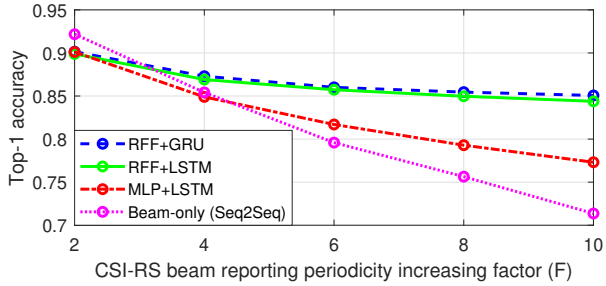

Fig. 4. Top-1 accuracy for different models vs CSI-RS reporting periodicity increasing factor (F)

RFF+GRU models, which use RFF layer to embed the location updates from the LiDAR data perform better compared to the other models. They reach top-1 accuracy values of 85% and 84.7% respectively even when $F = 10$. Interestingly, the beam-only model delivers the highest accuracy among all the models when $F = 2$. However, the top-1 accuracy of the beam-only model deteriorates drastically as the periodicity increases with F. Thus, the potential of the location updates to aid in increasing the BMR interval is evident. Similarly, the MLP+LSTM model performs comparably to the other RNN models when $F = 2$. However, the performance decreases as F increases compared to the RFF equipped models. The reason behind this is, the MLP layer does not embed the location data in an efficient manner although the location data from LiDAR is utilized to support the prediction. Therefore, we can notice the importance of utilizing the location data and its efficient embedding using the RFF layer. The models with the RFF layer have the ability to rely entirely on the location updates, resulting in a noticeable performance improvement compared to the other models with its efficient location embedding. The performance difference between RFF+LSTM and RFF+GRU models is negligible in this case and the RFF+GRU model achieves slightly a better accuracy with less number of parameters. Hence, we can conclude that the proposed model, RFF+GRU provides a significant accuracy using lesser parameters with infrequent BMR by relying on the location data from the LiDARs.

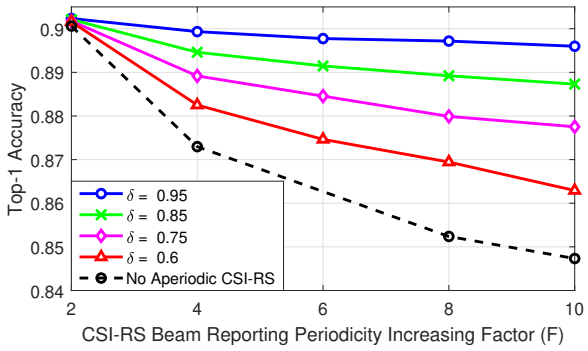

Fig. 5. Variation of top-1 accuracy with threshold vs CSI-RS beam reporting periodicity increasing factor (F)

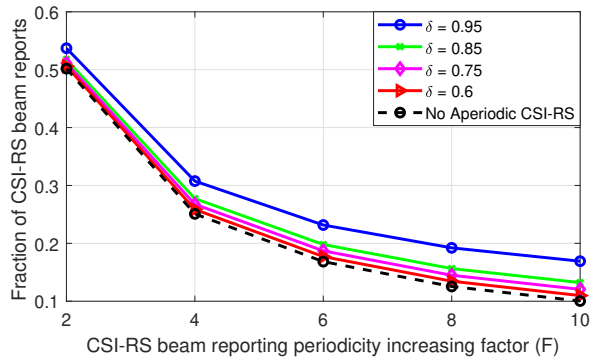

Fig. 6. Fraction of CSI-RS beam reports with δ vs CSI-RS beam reporting periodicity increasing factor (F)

Then we analyze the effect of using aperiodic CSI-RS BMR to further refine the proposed method as described in Section III-C. The RFF+GRU model is used in these simulations. We use threshold values $\delta \in \{0.6, 0.75, 0.85, 0.95\}$ and the variation of top-1 accuracy with F is shown in Figure 5. Clearly, the top-1 accuracy in Figure 5 improves when the aperiodic CSI-RS BMRs are used, compared to the case of not using them. Naturally, all the top-k accuracy values increase with this approach, although we have shown only the top-1 accuracy. The improvement in the accuracy comes at the expense of increased resource usage. To analyze this, we plot the fraction of the CSI-RS BMRs used with each δ value, against the increasing F in Figure 6. The fraction in this context means the total number of beams scheduled for the report with both periodic and aperiodic BMRs with a corresponding F and δ, divided by the total number of BMRs that would have been used, if there was no predictive mechanism. In other words, it reflects the amount of resources used by the predictive mechanism compared to the conventional BMRs. When the δ is set to a higher level at 0.95, the model decision is scrutinized by an increase of 7% aperiodic beams compared to the no aperiodic BMR case when $F = 10$. Note that, we

focus on a higher F because it gives the maximum resource saving, which was our primary objective. The benefit of using a higher δ is the improvement in top-1 accuracy to 89.6%, with the cost of increased resource usage. The considered lower values of δ, 0.6 and 0.75 give a top-1 accuracy improvement of nearly 1.6% and 3%, while increasing the BMR fraction by 1% and 2.1% respectively. The δ value of 0.85 strikes a balance between the accuracy and resource usage since it provides an increased accuracy of 88.7% while only using a 3.2% increase in resource usage for aperiodic BMRs when $F = 10$. Nevertheless, the subset of beams to be scheduled for these aperiodic BMRs are minimal, which is evident from the Figure 6 as we have relatively small increments ($\leq 7\%$) in the fraction of CSI-RS BMRs for all the δ values. It is worthwhile to note that the value of δ will depend on the requirements of the application. If more reliability is needed, a higher δ should be used at the expense of high resources usage. Otherwise a lower δ value can be used compromising reliability to save maximum amount of resources.

Single-antenna UEs were considered in the study due to the prohibitively high computation time of ray-tracing for the considered scenario. However, UEs with multiple-antennas capable of UE-side beam refinement will be considered in the future studies. Furthermore, the results analyzed in this work contained perfect detection and tracking in the LiDAR point clouds with the simplicity of the simulation scenario. In a practical situation, detection errors and missing of tracking data of users can occur and the robustness of the model to rely on the BMRs needs to be evaluated in such a case. Moreover, the considered scenario had LOS for majority of the time instances and the performance under NLOS will be a direction of future work.

VI. Conclusions

This paper proposed a method for beam prediction for a 5G NR UE based on a co-existing infrastructure-mounted LiDAR system in an indoor hotspot scenario. The system utilizes the LiDAR data to detect and track the users, which provides a trajectory history. The trajectory and beam sequence history were used to predict the future beam index for a certain user using an RNN model. The model consists of an RFF layer which encodes the trajectory data efficiently while a GRU layer is used to capture the sequential nature of the data. Furthermore, a predictive beam management method utilizing the proposed model to increase the periodicity of the reports and trigger on demand aperiodic reports was analyzed. The results demonstrated that the proposed method achieves an acceptable accuracy while saving a significant amount of resources. This shows utilizing LiDARs with the network can be useful to enable efficient beam-based operation with very low over-the-air signaling overhead, which is promising for a 5G NR system. However, a more comprehensive system specific study with dynamic simulations are needed to understand the true 5G NR system gains, which will be the scope of further work.

References

[1] M. Enescu, *5G New Radio: A Beam-based Air Interface*. Wiley, 2020.

[2] 3GPP, "Study on Integrated Sensing and Communication," 3rd Generation Partnership Project (3GPP), New SID, Feb. 2022.

[3] ——, "Study on Artificial Intelligence (AI)/Machine Learning (ML) for NR Air Interface," 3rd Generation Partnership Project (3GPP), New SID, Dec. 2021.

[4] N. Jayaweera, N. Rajatheva, and M. Latva-aho, "Autonomous Driving without a Burden: View from Outside with Elevated LiDAR," in *2019 IEEE 89th Vehicular Technology Conference (VTC2019-Spring)*, 2019, pp. 1–7.

[5] N. Jayaweera, D. Marasinghe, *et al.*, "Factory Automation: Resource Allocation of an Elevated LiDAR System with URLLC Requirements," in *2020 2nd 6G Wireless Summit (6G SUMMIT)*, 2020, pp. 1–5.

[6] D. Marasinghe, N. Rajatheva, and M. Latva-aho, "LiDAR Aided Human Blockage Prediction for 6G," in *2021 IEEE Globecom Workshops (GC Wkshps)*, 2021, pp. 1–6.

[7] A. Klautau, N. González-Prelcic, and R. W. Heath, "LIDAR data for deep learning-based mmWave beam-selection," *IEEE Wireless Communications Letters*, vol. 8, no. 3, pp. 909–912, 2019.

[8] M. Dias, A. Klautau, *et al.*, "Position and LiDAR-Aided mmWave Beam Selection using Deep Learning," in *2019 IEEE 20th International Workshop on Signal Processing Advances in Wireless Communications (SPAWC)*, 2019, pp. 1–5.

[9] M. Zecchin, M. B. Mashhadi, *et al.*, "LIDAR and Position-Aided mmWave Beam Selection with Non-local CNNs and Curriculum Training," 2021. arXiv: 2104.14579.

[10] M. Alrabeiah, A. Hredzak, and A. Alkhateeb, "Millimeter Wave Base Stations with Cameras: Vision Aided Beam and Blockage Prediction," 2019. arXiv: 1911.06255.

[11] Z. Ying, H. Yang, *et al.*, "A New Vision-Aided Beam Prediction Scheme for mmWave Wireless Communications," in *2020 IEEE 6th International Conference on Computer and Communications (ICCC)*, 2020, pp. 232–237.

[12] A. Ö. Kaya and H. Viswanathan, "Deep Learning-based Predictive Beam Management for 5G mmWave Systems," in *2021 IEEE Wireless Communications and Networking Conference (WCNC)*, 2021, pp. 1–7.

[13] M. Padmal, D. Marasinghe, *et al.*, "Elevated LiDAR based Sensing for 6G – 3D Maps with cm Level Accuracy," 2021. arXiv: 2102.10849.

[14] K. Koide, J. Miura, and E. Menegatti, "A portable three-dimensional LiDAR-based system for long-term and wide-area people behavior measurement," *International Journal of Advanced Robotic Systems*, vol. 16, no. 2, 2019.

[15] M. Häselich, B. Jöbgen, *et al.*, "Confidence-based pedestrian tracking in unstructured environments using 3D laser distance measurements," in *2014 IEEE/RSJ International Conference on Intelligent Robots and Systems*, 2014, pp. 4118–4123.

[16] Luc Le Magoarou and Taha Yassine and Stéphane Paquelet and Matthieu Crussière, "Deep learning for location based beamforming with nlos channels," 2021. arXiv: 2201.01386.

[17] 3rd Generation Partnership Project, "Study on Scenarios and Requirements for Next Generation Access Technologies (3GPP TR 38.913 version 14.2.0 Release 14)," 2017.

[18] M. Gschwandtner, R. Kwitt, *et al.*, "Blensor: Blender sensor simulation toolbox," G. Bebis, R. Boyle, *et al.*, Eds., pp. 199–208, 2011.

[19] Wireless InSite, *Remcom Inc.* 2021.

[20] J. van den Berg, M. Lin, and D. Manocha, "Reciprocal Velocity Obstacles for real-time multi-agent navigation," in *2008 IEEE International Conference on Robotics and Automation*, 2008, pp. 1928–1935.